

A parameterised family of neuralODEs optimally fitting steady-state data

M.F. Shakib, G. Scarciozzi, A. Astolfi

Abstract—This paper presents a parameterised family of neural ordinary differential equations (neuralODEs) that fit the *steady-state* system response in a least-squares sense. The family of neuralODEs is cast in the form of recurrent equilibrium networks (NodeRENs). One of the main advantages of the proposed approach is that it uses only linear least-squares optimisation tools. As such, the solution to the steady-state fitting problem is given in a closed-form expression. Furthermore, the NodeREN family leaves a subset of parameters free. This is useful for enforcing robustness or for fitting transient data in addition to steady-state data.

I. INTRODUCTION

The notion of *steady-state* response [1] plays a central role in the analysis and design of control systems. For a linear time-invariant (LTI) system, the steady-state response is closely related to its frequency-response function (FRF). This has led to the development of frequency-domain analysis and design techniques for LTI systems [2]. Beyond LTI systems, the steady-state response has also been instrumental in the analysis and design of nonlinear systems. For example, this notion has been used for the performance optimisation of nonlinear control systems in the form of Lur’e-type systems [3] and hybrid-integrator-gain systems [4]. Dynamic models that capture the steady-state response of (nonlinear) systems are therefore essential for the analysis and model-based design of nonlinear control systems.

Deriving dynamic models that capture steady-state behaviour can be a challenging task and, given the complexity of today’s engineering systems, often results in overly complex models. Alternatively, data-driven modelling approaches exploit data to directly construct dynamic models that closely fit the data. Such data can either be collected experimentally from a data-generating system or generated by a high-complexity model. The construction of LTI models that capture the steady-state system response of an LTI system is well understood [5], [6], [7]. However, constructing models for nonlinear systems that capture the steady-state behaviour or at least ensure a close fit to data collected from the steady-state system behaviour is much more challenging [8].

A particular class of nonlinear models is the class of neural ordinary differential equations (neuralODEs) [9]. These

models exploit the expressive power of neural networks to learn the dynamics of complex systems from data. Recently, it has been shown that a large class of neuralODEs can be cast in the form of NodeRENs [10], a continuous-time counterpart of the discrete-time RENs [11]. NodeRENs and neuralODEs are typically trained using (stochastic) gradient-descent optimisers, such as the ADAM optimiser [12]. This has two drawbacks. First, the computation of the steady-state model response and its gradients is computationally expensive [13] due to the initial value problem that must be solved using numerical forward integration methods. Second, the gradient-descent training and the quality of the resulting NodeREN are highly dependent on the quality of the initialisation of the NodeREN parameters [14].

Widely used initialisation methods for neural networks randomly draw parameters from specific distributions, e.g., the uniform, standard, or Xavier distribution [15], as is done for NodeRENs in [10]. In these cases, the available data is not used for initialisation. Alternatively, [16] uses the data to construct the so-called best linear approximation of a nonlinear system. This approach, when applied to NodeRENs, results in a linear model. By definition, such a linear model does not capture the essential nonlinear behaviour. Consequently, the problem of constructing NodeRENs that optimally fit a given steady-state response is still open.

In this paper, we present a method for constructing a family of neuralODEs in the form of NodeRENs directly from data, such that each NodeREN in the family fits the steady-state system response in a least-squares sense. Using time-domain moment-matching theory [17], this proposed method involves only solving a linear least-squares problem. This problem has a closed-form solution that can be computed using reliable numerical algebra tools. This is in contrast to the time-consuming, gradient-descent learning process for which there are generally no optimality guarantees. The family of NodeRENs presented here also features parametric freedom, which can be used to enforce additional model properties such as stability. Alternatively, reminiscent of the problem in [18], this parametric freedom can be used to initiate a gradient-descent learning process to learn the free parameters such that, in addition to the steady-state response, the transient response is also fitted.

The constructed NodeREN family can be used for several applications. First, it can be used directly in the analysis and design of nonlinear control systems, e.g., to predict steady-state system responses to new inputs that were unseen in the construction process. Second, it can be used to warm start a stochastic gradient-descent algorithm for traditional data-driven learning of NodeRENs, where the initialiser is

M.F. Shakib, G. Scarciozzi, A. Astolfi are with the Department of Electrical and Electronic Engineering, Imperial College London, London, UK ({m.shakib; g.scarciozzi; a.astolfi}@imperial.ac.uk)

This work has been partially supported by the European Union’s Horizon 2020 Research and Innovation Programme under grant agreement No. 739551 (KIOS CoE); by the Italian Ministry for Research in the framework of the 2020 Program for Research Projects of National Interest (PRIN), Grant 2020RTWES4; and by the EPSRC grants EP/W005557 and EP/X033546.

close to a (locally) optimal point. Finally, it can be used as a reduced-complexity model in a data-driven model reduction problem, where the dataset is generated by a high-complexity model. In summary, the main contribution of this paper is a parameterised family of NodeRENs that fit given steady-state system data in a least-squares optimal sense. Numerical simulations are used to illustrate the results.

The remainder of this paper is structured as follows. Section II formally introduces the data-driven modelling problem studied, while Section III recalls the moment-matching theory. Section IV presents the proposed family of NodeRENs. Section V describes the results of a simulation study. Finally, Section VI presents some conclusions. All proofs are omitted due to space limitations.

Notation: The symbols \mathbb{R} , \mathbb{C} , and \mathbb{C}^- denote the set of real numbers, complex numbers, and complex numbers with a negative real part, respectively. The symbol \mathbb{T}^n denotes the set of strictly lower-triangular matrices of dimension $n \times n$. The symbol I_n denotes the $n \times n$ identity matrix. The spectrum of a matrix $A \in \mathbb{R}^{n \times n}$ is denoted by $\lambda(A)$. A symmetric matrix $A \in \mathbb{R}^{n \times n}$ is called positive (negative) definite, denoted by $A \succ 0$ ($A \prec 0$), if all its eigenvalues are strictly positive (negative). For a vector $x \in \mathbb{R}^n$, its Euclidean norm is denoted by $|x|$. For $T > 0$, $PC([0, T], \mathbb{R}^m)$ is the space of piecewise-continuous functions in the interval $[0, T]$, such that $u(t) \in \mathbb{R}^m$ for any $u \in PC([0, T], \mathbb{R}^m)$.

II. THE STEADY-STATE FITTING PROBLEM

Consider the unknown data-generating system described by the equations

$$\dot{x} = f(x, u), \quad y = h(x, u), \quad (1)$$

where f and h are smooth mappings and, at time instance $t \in \mathbb{R}$, $x(t) \in \mathbb{R}^n$ is the system state, $u(t) \in \mathbb{R}^m$ is the system input, and $y(t) \in \mathbb{R}^p$ is the system output. The dataset \mathcal{D} consists of N samples of the input $u_k := u(t_k)$ and of the system output $y_k := y(t_k)$, i.e.,

$$\mathcal{D} := \{u_k, y_k\}_{k=1}^N, \quad (2)$$

at time instants t_k , $k = 1, \dots, N$, which may be non-uniformly spaced.

To model the dynamics of (1), one could consider neural networks to approximate the mappings f and h . We consider the class of NodeRENs \mathcal{M} described by the equations

$$\mathcal{M}(\theta) : \begin{cases} \begin{bmatrix} \dot{\hat{x}} \\ \hat{v} \\ \hat{y} \end{bmatrix} = \begin{bmatrix} \hat{A} & \hat{B}_1 & \hat{B}_2 \\ \hat{C}_1 & \hat{D}_{11} & \hat{D}_{12} \\ \hat{C}_2 & \hat{D}_{21} & \hat{D}_{22} \end{bmatrix} \begin{bmatrix} \hat{x} \\ \hat{w} \\ u \end{bmatrix}, \\ \hat{w} = \sigma(\hat{v}) \in \mathbb{R}^{\hat{q}}, \end{cases} \quad (3)$$

where $\hat{x}(t) \in \mathbb{R}^{\hat{n}}$, $\hat{y}(t) \in \mathbb{R}^{\hat{p}}$, $u(t) \in \mathbb{R}^m$, $\hat{v}(t) \in \mathbb{R}^{\hat{q}}$ and $\hat{w}(t) \in \mathbb{R}^{\hat{q}}$, and all matrices have appropriate dimensions. The scalar activation function $\sigma : \mathbb{R} \rightarrow \mathbb{R}$ is applied element-wise to the components of the vector \hat{v} . The NodeREN parameters are collected in the set $\theta \in \mathbb{R}^{n_\theta}$. The quality of the model fit is assessed by a scalar loss function $\mathcal{L}(\theta, \mathcal{D})$.

We select this as the mean-square error (MSE) function, i.e.,

$$\mathcal{L}(\theta, \mathcal{D}) = \frac{1}{N} \sum_{k=1}^N |y_k - \hat{y}_k|^2, \quad (4)$$

where $\hat{y}_k := \hat{y}(t_k)$ is the sampled model output for the same input u . Given the NodeREN model class \mathcal{M} parameterised by θ and the dataset \mathcal{D} , the data-driven modelling problem is to find a specific model $\hat{\theta}$ from the class \mathcal{M} such that the scalar loss function $\mathcal{L}(\theta, \mathcal{D})$ is minimised.

Consider now an input that is periodic with period $T > 0$, i.e., $u(t) = u(t+T)$. Then, under suitable conditions on (1) (which we pose below), the output of the data-generating system (1) converges to a steady-state solution denoted by y_{ss} . Suppose that the duration of the experiment is sufficiently long such that the system output y reaches the steady-state output y_{ss} with sufficient accuracy. Then, loosely speaking, the dataset \mathcal{D} can be split into a part containing $N - N_{ss}$ samples of the transient response \mathcal{D}_{tr} and a part containing N_{ss} samples of the steady-state response \mathcal{D}_{ss} . The loss function \mathcal{L} in (4) can then be decomposed into a part that accounts for the transient response (\mathcal{L}_{tr}) and a part that accounts for the steady-state response (\mathcal{L}_{ss}) as

$$\mathcal{L}(\theta, \mathcal{D}) \approx \mathcal{L}_{tr}(\theta, \mathcal{D}_{tr}) + \mathcal{L}_{ss}(\theta, \mathcal{D}_{ss}). \quad (5)$$

The problem considered in this paper is to provide a parameterisation Θ_{ss} of a family of NodeRENs \mathcal{M} such that for any $\theta \in \Theta_{ss}$, the corresponding NodeREN $\mathcal{M}(\theta)$ i) is well-posed, i.e., has a unique solution for any $u \in PC([0, \infty], \mathbb{R}^m)$ and $x(0) \in \mathbb{R}^{\hat{n}}$; ii) has a locally exponentially stable origin for zero input; and iii) achieves a ‘small’ loss \mathcal{L}_{ss} on the steady-state dataset \mathcal{D}_{ss} .

Remark 1: The NodeRENs in [10] have a bias term in the \hat{x} , \hat{v} , and \hat{y} equations. Since this paper only considers the local behaviour around the origin, we do not consider the bias terms, although the results can be trivially extended to accommodate bias terms.

III. MOMENT-MATCHING THEORY RECALLED

This section recalls the moment-matching theory for nonlinear systems from [17]. Consider a signal generator described by the equations

$$\dot{\underline{x}} = s(\underline{x}), \quad u = \ell(\underline{x}), \quad (6)$$

where $\underline{x}(t) \in \mathbb{R}^{\underline{n}}$ and $u(t) \in \mathbb{R}^m$, and $s : \mathbb{R}^{\underline{n}} \rightarrow \mathbb{R}^{\underline{n}}$ and $\ell : \mathbb{R}^{\underline{n}} \rightarrow \mathbb{R}^m$ are smooth mappings. Furthermore, consider the interconnection between the data-generating system (1) and the signal generator (6), i.e., the system:

$$\dot{\underline{x}} = s(\underline{x}), \quad (7a)$$

$$\dot{x} = f(x, \ell(\underline{x})), \quad (7b)$$

$$y = h(x, \ell(\underline{x})). \quad (7c)$$

We assume that the origin of (7) is an equilibrium, i.e., $f(0, 0) = 0$ and $h(0, 0) = 0$, and that $s(0) = 0$ and $\ell(0) = 0$.

Under a set of assumptions (see [19]) on both the data-generating system (1) and the signal generator (6), the interconnected system (7) possesses an invariant manifold.

Assumption 1: The mappings f and h are twice continuously differentiable and the origin of the system (1) is locally exponentially stable, i.e., $\partial f/\partial x(0,0)$ is Hurwitz.

Assumption 2: The signal generator (6) is neutrally stable.

Lemma 2 ([20]): Consider the interconnection (7). Suppose that the Assumptions 1 and 2 hold. Then there exists a mapping π , locally defined in a neighbourhood of $\underline{x} = 0$, which solves the partial differential equation

$$\frac{\partial \pi(\underline{x})}{\partial \underline{x}} s(\underline{x}) = f(\pi(\underline{x}), \ell(\underline{x})) \quad (8)$$

In addition, for any sufficiently small $x(0)$ and $\underline{x}(0)$, the steady-state response x_{ss} of the system (1) is $\pi(\underline{x})$.

By Lemma 2, there exists a mapping that maps the state \underline{x} of the signal generator to the steady-state response x_{ss} of the system (1) for the interconnection (7). A family of models that exhibit a steady-state output that matches the steady-state output of the system (1) for the input generated by (6), i.e., $\hat{y}_{ss} = y_{ss} = h(\pi(\underline{x}), \ell(\underline{x}))$, is described by the equations

$$\begin{aligned} \dot{\hat{x}} &= s(\hat{x}) - \delta(\hat{x}, \ell(\hat{x})) + \delta(\hat{x}, u), \\ \hat{y} &= h(\pi(\hat{x}), \ell(\hat{x})) - \kappa(\hat{x}, \ell(\hat{x})) + \kappa(\hat{x}, u), \end{aligned} \quad (9)$$

where $\kappa : \mathbb{R}^\nu \times \mathbb{R}^m \rightarrow \mathbb{R}^\nu$ is a free mapping and $\delta : \mathbb{R}^\nu \times \mathbb{R}^m \rightarrow \mathbb{R}^\nu$ is any mapping such that

$$\frac{\partial r}{\partial \underline{x}} s(\underline{x}) = s(r(\underline{x})) - \delta(r(\underline{x}), \ell(r(\underline{x}))) + \delta(r(\underline{x}), \ell(\underline{x})), \quad (10)$$

has the unique solution $r(\underline{x}) = \underline{x}$. The model (9) has the same state dimension ν as the signal generator (6). Therefore, the dimension ν should be chosen to match the required state dimension n of the data-driven model (9).

There are two challenges to using the moment-matching theory in the context of learning NodeRENs. First, it is unclear how to select the mappings s and ℓ in (6) and the free mappings δ and κ such that the resulting model (9) is of NodeREN form and satisfies Assumption 2 and equation (10). Second, the mapping f of the data-generating system (1) should be known in order to solve the partial differential equation (8). Even if f was known, solving (8) would be a non-trivial and rather case-specific task. In the problem at hand, however, the mapping f is unknown, hence we have to resort to a *data-driven* moment-matching approach [20].

Remark 3: Under stricter assumptions, Lemma 2 can be extended in which π exists globally, see [21] for more details.

IV. FAMILY OF NODERENS FITTING STEADY-STATE DATA

This section presents a family of NodeRENs that fits given steady-state data in a least-squares sense. First, we recall sufficient conditions for NodeRENs to be contractive, a global notion of stability. This notion is subsequently used in Section IV-B to present a class of NodeREN signal generators. Then, Sections IV-C and IV-D use the moment-matching theory of Section III to construct a parameterised family of NodeRENs that fit the steady-state output response.

A. Contracting RENs

We recall the definition of contraction and sufficient conditions for contraction from [10]. A sufficient condition for

well-posedness is that the matrix \hat{D}_{11} is a strictly lower-triangular matrix [10], i.e., $\hat{D}_{11} \in \mathbb{T}^{\hat{q}}$.

Definition 4 ([10, Definition 1]): The NodeREN (3) is said to be contracting if for any two initial conditions $\hat{x}^a(0) \in \mathbb{R}^{\hat{n}}$ and $\hat{x}^b(0) \in \mathbb{R}^{\hat{n}}$ and input signal $u \in PC([0, T], \mathbb{R}^m)$, the corresponding state trajectories \hat{x}^a and \hat{x}^b satisfy:

$$|\hat{x}^a(t) - \hat{x}^b(t)| \leq \eta e^{-ct} |\hat{x}^a(0) - \hat{x}^b(0)|, \quad (11)$$

for all $t \geq 0$ and some constants $0 \leq \eta < +\infty$ and $0 \leq c < +\infty$.

Assumption 3: The slope of the scalar activation function σ in (3) is restricted to the interval $[0, 1]$, i.e.,

$$0 \leq \frac{\sigma(v_1) - \sigma(v_2)}{v_1 - v_2} \leq 1, \quad \forall v_1 \in \mathbb{R}, v_2 \in \mathbb{R}, v_1 \neq v_2. \quad (12)$$

Theorem 5 ([10, Theorem 1]): Consider NodeREN (3) and suppose that Assumption 3 holds and $\hat{D}_{11} \in \mathbb{T}^{\hat{q}}$. If there exists a symmetric positive-definite matrix $P \in \mathbb{R}^{\hat{n}}$ and a diagonal positive-definite matrix $\Lambda \in \mathbb{R}^{\hat{q}}$ such that

$$\begin{bmatrix} -\hat{A}^\top P - P\hat{A} & -\hat{C}_1^\top \Lambda - P\hat{B}_1 \\ * & 2\Lambda - \Lambda D_{11} - D_{11}^\top \Lambda \end{bmatrix} \succ 0, \quad (13)$$

then the NodeREN (3) is contracting.

The work in [10] provides a direct parameterisation of NodeRENs (3) that are contracting. We will use the direct parameterisation to construct signal generators that produce periodic and bounded input signals.

For the main results in this paper, we require a more restrictive smoothness assumption on the activation functions.

Assumption 4: The scalar activation function σ in (3) is twice continuously differentiable and its derivative is restricted to the interval $[0, 1]$, i.e.,

$$0 \leq \frac{\partial \sigma}{\partial v}(v) \leq 1, \quad \forall v \in \mathbb{R}. \quad (14)$$

This assumption is satisfied for the tanh and sigmoid activation functions, but not for non-smooth activation functions. Note that Assumption 4 implies Assumption 3.

B. Input design via a NodeREN signal generator

The proposed signal generator consists of the interconnection between a linear harmonic oscillator and a contracting NodeREN, see Figure 1. The oscillator is described by

$$\dot{\tilde{\tau}} = \tilde{S}\tilde{\tau}, \quad \tilde{u} = \tilde{L}\tilde{\tau}, \quad (15)$$

where $\tilde{\tau}(t) \in \mathbb{R}^{n_{\tilde{\tau}}}$, $\tilde{u}(t) \in \mathbb{R}^{n_{\tilde{u}}}$, $\tilde{S} \in \mathbb{R}^{n_{\tilde{\tau}} \times n_{\tilde{\tau}}}$ and $\tilde{L} \in \mathbb{R}^{n_{\tilde{u}} \times n_{\tilde{\tau}}}$. For example, the choice

$$\tilde{S} = \begin{bmatrix} 0 & 2\pi f_0 \\ -2\pi f_0 & 0 \end{bmatrix}, \quad (16)$$

generates a harmonic signal with frequency $f_0 \in \mathbb{R}$ in Hz.

The contracting NodeREN is constructed using the procedure in [10, Section III.B] and is given by the equations

$$\begin{bmatrix} \dot{\tilde{x}} \\ \tilde{v} \\ u \end{bmatrix} = \begin{bmatrix} \tilde{A} & \tilde{B}_1 & \tilde{B}_2 \\ \tilde{C}_1 & \tilde{D}_{11} & \tilde{D}_{12} \\ \tilde{C}_2 & \tilde{D}_{21} & \tilde{D}_{22} \end{bmatrix} \begin{bmatrix} \tilde{x} \\ \tilde{w} \\ \tilde{u} \end{bmatrix}, \quad (17)$$

$$\tilde{w} = \sigma(\tilde{v}) \in \mathbb{R}^{\tilde{q}},$$

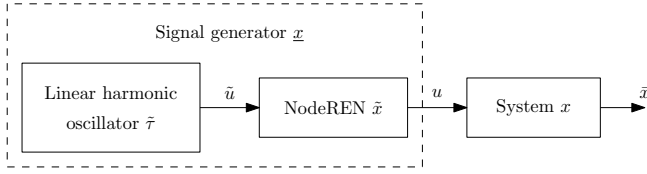


Fig. 1. The interconnection between the linear harmonic oscillator (15), the NodeREN (17), and the system (1). The signal generator is the interconnection between the linear harmonic oscillator and NodeREN.

where $\tilde{x}(t) \in \mathbb{R}^{n_{\tilde{x}}}$, $\tilde{u}(t) \in \mathbb{R}^{\tilde{m}}$, $\tilde{v}(t) \in \mathbb{R}^{\tilde{q}}$, $\tilde{w}(t) \in \mathbb{R}^{\tilde{q}}$, and $u(t) \in \mathbb{R}^m$. The matrix $\tilde{D}_{11} \in \mathbb{T}^{\tilde{q}}$ is a strictly lower-triangular matrix to ensure well-posedness, and the remaining matrices have appropriate dimensions.

Consider the interconnection between (15) and (17) and note that it is again a NodeREN with the extended state $\underline{x}^\top = [\tilde{\tau}^\top \ \tilde{x}^\top] \in \mathbb{R}^{1 \times n}$, $\underline{n} := n_{\tilde{\tau}} + n_{\tilde{x}}$, i.e., the system

$$\begin{bmatrix} \dot{\underline{x}} \\ \underline{v} \\ \underline{u} \end{bmatrix} = \begin{bmatrix} \underline{A} & \underline{B}_1 \\ \underline{C}_1 & \underline{D}_{11} \\ \underline{C}_2 & \underline{D}_{21} \end{bmatrix} \begin{bmatrix} \underline{x} \\ \underline{w} \end{bmatrix}, \quad (18)$$

$$\underline{w} = \sigma(\underline{v}) \in \mathbb{R}^{\tilde{q}},$$

where

$$\begin{bmatrix} \underline{A} & \underline{B}_1 \\ \underline{C}_1 & \underline{D}_{11} \\ \underline{C}_2 & \underline{D}_{21} \end{bmatrix} := \begin{bmatrix} \tilde{S} & 0 & 0 \\ \tilde{B}_2 \tilde{L} & \tilde{A} & \tilde{B}_1 \\ \tilde{D}_{12} \tilde{L} & \tilde{C}_1 & \tilde{D}_{11} \\ \tilde{D}_{22} \tilde{L} & \tilde{C}_2 & \tilde{D}_{21} \end{bmatrix}. \quad (19)$$

This signal generator can be trivially cast in the form of (6). To simplify the presentation of some results, we sometimes make use of the following assumption.

Assumption 5: The matrix \underline{D}_{21} in (19) is the zero matrix.

Next, we show that there exists a mapping that maps the steady-state response \underline{x}_{ss} of the signal generator (18) to the steady-state response x_{ss} of the system (1). Hereto, we pose the following assumptions on the linear harmonic oscillator and the contracting NodeREN.

Assumption 6: Suppose that

- A) the eigenvalues of \tilde{S} in (15) are simple and located on the imaginary axis;
- B) the NodeREN (17) satisfies the condition of Theorem 5 and is therefore contracting.

Assumption A) implies that the linear harmonic oscillator satisfies Assumption 2. Assumption B) implies global exponential stability of the origin of the NodeREN for zero input. Note that Assumption 6 can be trivially satisfied by the design of the signal generator. The relationship between the steady-state responses \underline{x}_{ss} and x_{ss} is presented next.

Theorem 6: Consider system (1) driven by an input generated by the signal generator (18). Suppose Assumptions 1, 4, and 6 hold. Then, there exists a mapping $\pi : \mathbb{R}^n \rightarrow \mathbb{R}^n : \underline{x}_{ss} \mapsto x_{ss}$ such that for $x(0)$ and $\underline{x}(0)$ sufficiently small, the steady-state response x_{ss} is $\pi(\underline{x}_{ss})$.

The next section proposes a family of NodeRENs that exhibit a steady-state response \hat{x}_{ss} that coincides with \underline{x}_{ss} . The steady-state dataset \mathcal{D}_{ss} is then exploited in Section IV-D to parameterise a family of NodeRENs that fits the steady-state output y_{ss} of the system in a least-squares sense.

C. Family of NodeRENs that match the state of the signal generator

This section presents a family of NodeRENs that achieves the matching

$$x^* := \hat{x}_{ss} = \underline{x}_{ss}, \quad (20a)$$

$$w^* := \hat{w}_{ss} = \underline{w}_{ss}, \quad (20b)$$

i.e., the steady-state response \hat{x}_{ss} and the steady-state activation function output \hat{w}_{ss} of the NodeREN (3) match those of the signal generator (18). Taking the time derivative on both sides of (20a) gives the following condition:

$$\hat{A}x^* + \hat{B}_1 w^* + \hat{B}_2 u_{ss} = \underline{A}x^* + \underline{B}_1 w^*. \quad (21)$$

Substituting $u_{ss} = \underline{C}_2 x^* + \underline{D}_{21} w^*$ and collecting terms results in

$$\hat{A} = \underline{A} - \hat{B}_2 \underline{C}_2, \quad \hat{B}_1 = \underline{B}_1 - \hat{B}_2 \underline{D}_{21}, \quad (22)$$

where $\hat{B}_2 \in \mathbb{R}^{\hat{n} \times m}$ is a free matrix. Similarly, considering (20b), one has

$$\hat{C}_1 x^* + \hat{D}_{11} w^* + \hat{D}_{12} u_{ss} = \underline{C}_1 x^* + \underline{D}_{11} w^*.$$

Again, substituting $u_{ss} = \underline{C}_2 x^* + \underline{D}_{21} w^*$ and collecting terms results in the conditions

$$\hat{C}_1 = \underline{C}_1 - \hat{D}_{12} \underline{C}_2, \quad \hat{D}_{11} = \underline{D}_{11} - \hat{D}_{12} \underline{D}_{21}, \quad (23)$$

where $\hat{D}_{12} \in \mathbb{R}^{\hat{q} \times m}$ is a free matrix. The Jacobian of the dynamics of the NodeREN (3) is denoted by $\hat{J}(\hat{x}, u)$. The parameters \hat{B}_2 and \hat{D}_{12} can be used to enforce local exponential stability of the origin of the NodeREN, i.e., $\lambda(\hat{J}(0, 0)) \in \mathbb{C}^-$. To ensure that \hat{D}_{11} is a strictly lower-triangular matrix, we can trivially choose the matrix \underline{D}_{21} of the signal generator as the zero matrix (as in Assumption 5) or the matrix \hat{D}_{12} of the model as the zero matrix. The family of well-posed NodeRENs in the form of (3) that satisfy (20) and has a locally stable equilibrium at the origin is denoted by $\tilde{\Theta}$ and is defined as

$$\tilde{\Theta} := \{\theta \in \mathbb{R}^{n_\theta} \text{ such that } \hat{D}_{11} \in \mathbb{T}^{\hat{q}}, (22), (23), \lambda(\hat{J}(0, 0)) \in \mathbb{C}^-\}. \quad (24)$$

These results are summarised next.

Assumption 7: Suppose there exist a $\hat{B}_2 \in \mathbb{R}^{\hat{n} \times m}$ and $\hat{D}_{12} \in \mathbb{R}^{\hat{q} \times m}$ such that $\lambda(\hat{J}(0, 0)) \in \mathbb{C}^-$.

Lemma 7: Consider the signal generator (18) and the class of NodeRENs \mathcal{M} in (3). Suppose Assumptions 4, 6, and 7 hold. Then, the set $\tilde{\Theta}$ in (24) is non-empty and for any $\theta \in \tilde{\Theta}$, the solutions of the NodeREN $\mathcal{M}(\theta)$ are well-posed. Furthermore, for sufficiently small $\underline{x}(0)$ and $\hat{x}(0)$, the steady-state response \hat{x}_{ss} of $\mathcal{M}(\theta)$ driven by the input u generated by (18) satisfies the equalities (20).

D. Family of locally exponentially stable NodeRENs that achieve least-squares steady-state output matching

The parameter set $\tilde{\Theta}$ in (24) leaves \hat{C}_2 , \hat{D}_{21} , and \hat{D}_{22} free. These are found using the procedure in this section. The steady-state output of any NodeREN in $\tilde{\Theta}$ can be written as

$$\hat{y}_{ss} = \hat{C}_2 \underline{x}_{ss} + \hat{D}_{21} \underline{w}_{ss} + \hat{D}_{22} u_{ss}, \quad (25)$$

where the equalities (20) are used. Substituting $u_{ss} = \underline{C}_2 \underline{x}_{ss} + \underline{D}_{21} \underline{w}_{ss}$ in (25) results in

$$\hat{y}_{ss} = \underbrace{(\hat{C}_2 + \hat{D}_{22} \underline{C}_2)}_{\Xi \in \mathbb{R}^{p \times \hat{n}}} \underline{x}_{ss} + \underbrace{(\hat{D}_{21} + \hat{D}_{22} \underline{D}_{21})}_{\Omega \in \mathbb{R}^{p \times \hat{q}}} \underline{w}_{ss}. \quad (26)$$

The signals \underline{x}_{ss} and \underline{w}_{ss} are known as the signal generator (18) is user-defined. Therefore, finding Ξ and Ω boils down to solving a linear least-squares problem. To this end, we introduce the steady-state loss function

$$\mathcal{L}_{ss}(\alpha, \mathcal{D}_{ss}) := \frac{1}{N_{ss}} \sum_{k=1}^{N_{ss}} |y_{ss}(t_k) - \alpha^\top \phi(t_k)|^2, \quad (27)$$

where α and ϕ are defined as

$$\alpha := \begin{bmatrix} \Xi^\top \\ \Omega^\top \end{bmatrix} \in \mathbb{R}^{\hat{n} + \hat{q} \times p}, \quad \phi(t) := \begin{bmatrix} \underline{x}_{ss}(t) \\ \underline{w}_{ss}(t) \end{bmatrix} \in \mathbb{R}^{\hat{n} + \hat{q}}. \quad (28)$$

Then, the linear least-squares problem corresponding to the steady-state part of the loss function in (4) is

$$\hat{\alpha} = \arg \min_{\alpha \in \mathbb{R}^{p \times \hat{n} + \hat{q}}} \mathcal{L}_{ss}(\alpha, \mathcal{D}_{ss}) \quad (29)$$

with $\mathcal{L}_{ss}(\alpha, \mathcal{D}_{ss})$ as defined in (27). The global optimal solution of (29) has the closed-form expression $\hat{\alpha}^\top = Y \Phi^\top (\Phi \Phi^\top)^{-1}$, where $Y := [y_{ss}(t_1) \cdots y_{ss}(t_{N_{ss}})]$ and $\Phi := [\phi(t_1) \cdots \phi(t_{N_{ss}})]$.

After finding $\hat{\alpha}$, for any $\theta \in \tilde{\Theta}$ and selecting

$$\hat{C}_2 = \hat{\Xi} - \hat{D}_{22} \underline{C}_2, \quad \hat{D}_{21} = \hat{\Omega} - \hat{D}_{22} \underline{D}_{21}, \quad (30)$$

with $\hat{D}_{22} \in \mathbb{R}^{p \times m}$ a free matrix, the steady-state loss is

$$\hat{\mathcal{L}}_{ss} := \mathcal{L}_{ss}(\hat{\alpha}, \mathcal{D}_{ss}). \quad (31)$$

The optimisation problem (29) returns $\hat{\alpha}$, which defines \hat{C}_2 and \hat{D}_{21} via (30) and leaves \hat{D}_{22} free.

Finally, we present the family of models, denoted by Θ_{ss} , which achieves the steady-state error $\hat{\mathcal{L}}_{ss}$, that is

$$\Theta_{ss} := \{\theta \in \mathbb{R}^{n_\theta} \text{ such that } \hat{D}_{11} \in \mathbb{T}^{\hat{q}}, (22), (23), (30) \quad (32) \\ \lambda(\hat{J}(0,0)) \in \mathbb{C}^-\}.$$

The free parameters are the matrices \hat{B}_2 , \hat{D}_{12} , and \hat{D}_{22} . Note that $\Theta_{ss} \subset \tilde{\Theta}$, therefore, any model in Θ_{ss} satisfies (20). Next, we summarise these results.

Assumption 8: The matrix $\Phi \Phi^\top$ is invertible.

Theorem 8: Suppose Assumptions 1, 4, 6, 7, and 8 hold. Then, the set Θ_{ss} in (32) is non-empty. Furthermore, for sufficiently small $\underline{x}(0)$ and $\hat{x}(0)$, every NodeREN $\mathcal{M}(\theta)$ in (3) that is characterised by $\theta \in \Theta_{ss}$ and driven by (18) achieves the steady-state mismatch $\hat{\mathcal{L}}_{ss}$ in (31).

The free parameters \hat{B}_2 , \hat{D}_{12} , \hat{D}_{22} can be used to enforce additional properties such as contraction, passivity, or local stability. Here, we focus on local exponential stability. Under Assumption 5, the Jacobian $\hat{J}(0,0)$ of the NodeREN (3) is

$$\hat{J}(0,0) = \hat{A} + \hat{B}_1 \left(I_{\hat{q}} - \gamma \hat{D}_{11} \right)^{-1} \left(\gamma \hat{C}_1 \right), \quad (33)$$

where $\gamma := \partial \sigma / \partial \hat{v}(0)$ and σ is the activation function. The matrix inverse exists in (33) since \hat{D}_{11} is a strictly lower-

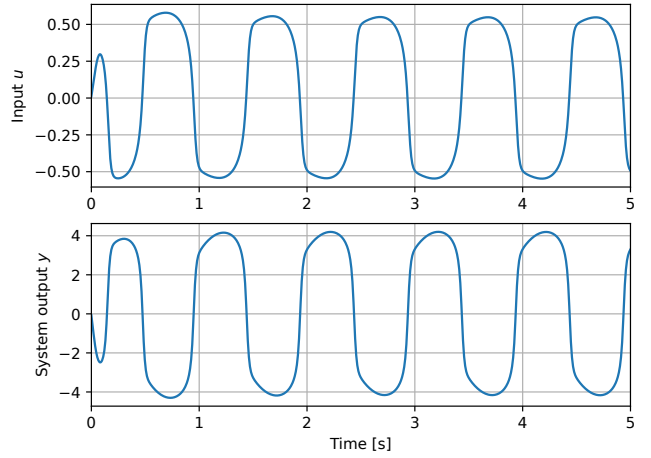


Fig. 2. Top graph: input signal generated by the NodeREN signal generator with a frequency of 1 Hz. Bottom graph: corresponding system output.

triangular matrix. Substituting \hat{A} and \hat{B}_1 from (22) and \hat{C}_1 from (23) into (33) yields

$$\hat{J}(0,0) = \underline{A} - \hat{B}_2 \underline{C}_2 \\ + \underline{B}_1 (I_{\hat{q}} - \gamma \underline{D}_{11})^{-1} (\gamma \underline{C}_1 - \hat{D}_{12} \underline{C}_2). \quad (34)$$

Consider a vector $p \in \mathbb{C}^{\hat{n}}$ with the desired poles location. By a poles placement argument, the observability of the pair

$$(\underline{A} + \underline{B}_1 (I_{\hat{q}} - \gamma \underline{D}_{11})^{-1} (\gamma \underline{C}_1 - \hat{D}_{12} \underline{C}_2), -\underline{C}_2)$$

for some $\hat{D}_{12} = \hat{D}_{12}^*$, is sufficient for the existence of a \hat{B}_2 such that $\lambda(\hat{J}(0,0)) = p$. Such a \hat{B}_2 and \hat{D}_{12} render the origin of the NodeREN (3) locally exponentially stable.

V. NUMERICAL CASE STUDY - NODEREN REDUCTION

This section presents a simulation study in which the proposed approach is used for complexity reduction. The data-generating system is a NodeREN with $n = 20$ and $q = 20$, and with tanh activation functions. This system is randomly sampled from a class of globally contractive NodeRENs using the procedure in [10, Section III.B]. The system thus satisfies Assumptions 1 and 4. We show that a NodeREN of lower order and containing a smaller number of neurons accurately fits the steady-state system output.

The signal generator is an interconnection of a second-order ($n_{\tilde{\tau}} = 2$) linear harmonic oscillator (15) and a contracting NodeREN (17), see Figure 1. The matrix \tilde{S} of the harmonic oscillator is chosen as in (16) with a frequency of $f_0 = 1$ Hz, while \tilde{L} is drawn from a normal distribution with unit variance. The contracting NodeREN is randomly drawn using the procedure in [10, Section III.B] with $n_{\tilde{x}} = 4$ and $\tilde{q} = 8$, and with $\underline{D}_{21} = 0$ to satisfy Assumption 5. The state dimension of the signal generator is then $\underline{n} = n_{\tilde{\tau}} + n_{\tilde{x}} = 6$ and the signal generator satisfies Assumption 6.

Figure 2 depicts the generated input u in the top graph and the system output y in the bottom graph. Based on the last period of this data, we solve the linear least-squares problem (29) using ridge regression with a small regularisation parameter. This gives the steady-state fit $\hat{\alpha}^\top \phi$ in Figure 3. This is an accurate fit as $\hat{\mathcal{L}}(\hat{\alpha})$ is $4.42 \cdot 10^{-3}$, while the mean-square value of y_{ss} is 13.12.

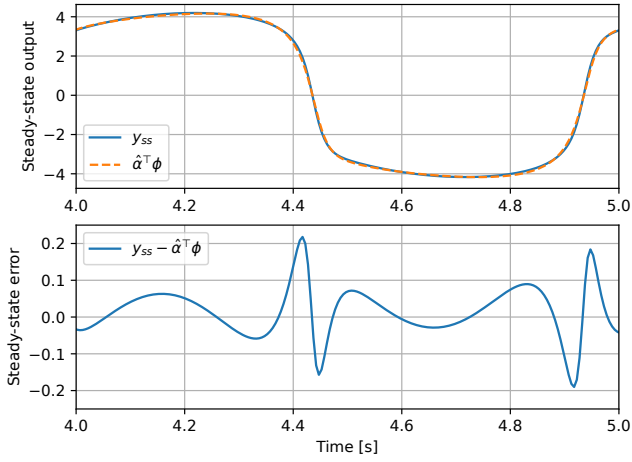


Fig. 3. Top graph: the steady-state system output and the linear least-squares fit $\hat{\alpha}^T \phi$. Bottom graph: the corresponding error between.

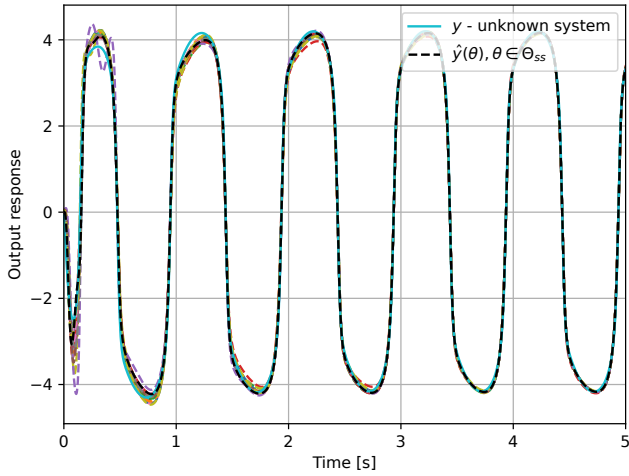


Fig. 4. The output response of 20 samples from the Θ_{ss} family of NodeRENs (represented by dashed lines). Their steady-state response closely matches the steady-state output of the data-generating system.

We use the following procedure to randomly draw a model from the family Θ_{ss} in (32). First, we draw the elements of the matrices \hat{B}_2 , \hat{D}_{12} , and \hat{D}_{22} from a normal distribution with unit variance. Then we select \hat{A} , \hat{B}_1 , \hat{C}_1 , \hat{D}_{11} , \hat{C}_2 , and \hat{D}_{21} according to (22), (23), and (30). Finally, we check whether the constraint $\lambda(\hat{J}(0,0)) \in \mathbb{C}^-$ is satisfied. If it is, then this is a random model from Θ_{ss} . If not, we repeat the procedure. Thanks to $\hat{D}_{21} = 0$, this procedure yields a strictly lower-triangular \hat{D}_{11} and thus satisfies all constraints in Θ_{ss} .

The response of 20 random NodeRENs from Θ_{ss} in (32) to the input in Figure 2 is depicted in Figure 4. It can be observed that after transients, the output of all models closely matches the steady-state system output. However, as can be seen in Figure 4, the transient response does not fit accurately for all of the selected models from the family Θ_{ss} . In our future work, we envision exploiting the freedom in the parameterisation of Θ_{ss} to also fit the transient data.

VI. CONCLUSIONS

This paper presents a parameterised family of NodeRENs that fit the *steady-state* model response to the *steady-state*

system response in a least-squares sense. The main advantage of the proposed approach is that it uses only *linear least-squares optimisation* for which there is a closed-form expression for the optimal solution. In a numerical example, we show that the steady-state response of models from this family does indeed converge to the steady-state response of the system. Future work includes using the method for data-driven learning of NodeRENs using transient and steady-state data and extending the method to the discrete-time case.

REFERENCES

- [1] A. Isidori and C. Byrnes, “Steady-state behaviors in nonlinear systems with an application to robust disturbance rejection,” *Annual Reviews in Control*, vol. 32, no. 1, pp. 1–16, 2008.
- [2] S. Skogestad and I. Postlethwaite, *Multivariable feedback control: analysis and design*, vol. 2. Wiley New York, 2007.
- [3] A. Pavlov, B. G. Hunnekens, N. v. Wouw, and H. Nijmeijer, “Steady-state performance optimization for nonlinear control systems of Lur’e type,” *Automatica*, vol. 49, no. 7, pp. 2087–2097, 2013.
- [4] D. A. Deenen, B. Sharif, S. van den Eijnden, H. Nijmeijer, M. Heemels, and M. Heertjes, “Projection-based integrators for improved motion control: Formalization, well-posedness and stability of hybrid integrator-gain systems,” *Automatica*, vol. 133, p. 109830, 2021.
- [5] L. Ljung, *System identification: theory for the user*. Prentice-Hall, Upper Saddle River, NJ, second ed., 1999.
- [6] R. Pintelon and J. Schoukens, *System identification: a frequency domain approach*. Hoboken, New Jersey, USA: Wiley & Sons Inc., 2012.
- [7] T. McKelvey, H. Akçay, and L. Ljung, “Subspace-based multivariable system identification from frequency response data,” *IEEE Transactions on Automatic Control*, vol. 41, no. 7, pp. 960–979, 1996.
- [8] M. F. Shakib, A. Y. Pogromsky, A. Pavlov, and N. van de Wouw, “Computationally efficient identification of continuous-time Lur’e-type systems with stability guarantees,” *Automatica*, vol. 136, p. 110012, 2022.
- [9] R. T. Chen, Y. Rubanova, J. Bettencourt, and D. K. Duvenaud, “Neural ordinary differential equations,” *Advances in neural information processing systems*, vol. 31, 2018.
- [10] D. Martinelli, C. L. Galimberti, I. R. Manchester, L. Furieri, and G. Ferrari-Trecate, “Unconstrained parametrization of dissipative and contracting neural ordinary differential equations,” *arXiv preprint arXiv:2304.02976*, 2023.
- [11] M. Revay, R. Wang, and I. R. Manchester, “Recurrent equilibrium networks: Flexible dynamic models with guaranteed stability and robustness,” *IEEE Transactions on Automatic Control*, pp. 1–16, 2023.
- [12] D. P. Kingma and J. Ba, “Adam: A method for stochastic optimization,” *arXiv preprint arXiv:1412.6980*, 2014.
- [13] F. Djeumou, C. Neary, E. Goubault, S. Putot, and U. Topcu, “Taylor-Lagrange neural ordinary differential equations: Toward fast training and evaluation of neural ODEs,” *arXiv preprint arXiv:2201.05715*, 2022.
- [14] D. Mishkin and J. Matas, “All you need is a good init,” *arXiv preprint arXiv:1511.06422*, 2015.
- [15] S. K. Kumar, “On weight initialization in deep neural networks,” *arXiv preprint arXiv:1704.08863*, 2017.
- [16] J. Schoukens, R. Pintelon, R. Dobrowiecki, and Y. Rolain, “Identification of linear systems with nonlinear distortions,” *Automatica*, vol. 41, no. 3, pp. 491–504, 2005.
- [17] A. Astolfi, “Model reduction by moment matching for linear and nonlinear systems,” *IEEE Transactions on Automatic Control*, vol. 55, no. 10, pp. 2321–2336, 2010.
- [18] G. Scarcioiti, Z. Jiang, and A. Astolfi, “Data-driven constrained optimal model reduction,” *European Journal of Control*, vol. 53, pp. 68–78, 2020.
- [19] G. Scarcioiti and A. Astolfi, “Nonlinear model reduction by moment matching,” *Foundations and Trends® in Systems and Control*, vol. 4, no. 3–4, pp. 224–409, 2017.
- [20] G. Scarcioiti and A. Astolfi, “Data-driven model reduction by moment matching for linear and nonlinear systems,” *Automatica*, vol. 79, pp. 340–351, 2017.
- [21] M. F. Shakib, G. Scarcioiti, A. Y. Pogromsky, A. Pavlov, and N. van de Wouw, “Model reduction by moment matching with preservation of global stability for a class of nonlinear models,” *Automatica*, vol. 157, p. 111227, 2023.